sciendo
ISSN 1335-8871
MEASUREMENT SCIENCE REVIEW
Journal homepage: https://content.sciendo.com

3-D Imaging Lidar Based on Miniaturized Streak Tube

Liping Tian[1,2], Lingbin Shen[1*], Yanhua Xue[2], Lin Chen[1], Ping Chen[2], Jinshou Tian[2], Wei Zhao[2].

[1]*School of network and communication engineering, Jinlin Institute of Technology, Hongjing Road, No.99, Nanjing, 211169, China, shen@jit.edu.cn*
[2]*Key Laboratory of Transient Optics and Photonics, Key Laboratory of Ultra-fast Photoelectric Diagnostics Technology, Xi'an Institute of Optics and Precision Mechanics, Chinese Academy of Sciences, Xinxi Road, No.17, Xi'an, 710119, China, xueyanhua@opt.ac.cn*

Abstract: Streak Tube Imaging Lidar (STIL), with advantages of non-scanning working mode, small distortion, high image framing rate, high resolution in low contrast environment, compact structure, easy miniaturization and high reliability, has a wide range of applications in military, aerospace, space confrontation, attack and defense, and marine law enforcement. This article introduces the principle of single-slit and multi-slit streak tube imaging lidar. It also introduces a single-slit general streak camera that can be used for imaging lidar. In addition, a multi-slit miniaturized streak tube with a single-lens focusing system with a total length of about 200 mm has been designed. The results of the 3D electromagnetic simulation show that the effective photocathode area of this streak tube reaches 36 mm × 36 mm, the temporal resolution is better than 50 ps, the dynamic spatial resolution can reach 12 lp/mm, and the whole photocathode can accommodate at least 19 slits in the effective detection range. The streak tube has a meshless structure, which is highly reliable. The streak tube can be used to increase the field of view of the imaging lidar system, improve the reliability, and achieve system miniaturization.

Keywords: Streak Tube Imaging Lidar (STIL), multi-slit streak tube, non-scanning, miniaturization.

1. INTRODUCTION

Streak Tube Imaging Lidar (STIL), which uses laser transmitters and streak tube receivers to obtain three-dimensional distance and one-dimensional intensity information of the target, is an active imaging system [1]-[3]. Compared with the traditional mechanical scanning lidar system, the STIL system has the advantage of small size, large field of view and light weight [4]-[5]. It can be widely used in aerospace, space confrontation, alien planet detection, underwater detection, ultraviolet missile warning, and other fields [6]-[9]. The performance of the STIL system depends heavily on the characteristics of the streak tube. For example, the detection Field Of View (FOV) is positively correlated with the effective photocathode working area and the spatial resolution in the slit direction [3]. The detection range is mainly determined by the photocathode radiation sensitivity and the transmission characteristics of the laser in the atmosphere. In addition, the miniaturization of the streak tube is also crucial for the overall miniaturization of the STIL system.

Since Knight et al. first demonstrated STIL with the single-slit streak tube detector in 1989, there have been several communities that have developed a variety of streak tubes suitable for STIL [10]. Research on single-slit streak tubes is mainly characterized by a large photocathode area, high spatio-temporal resolution, and small size [4]. The effective photocathode area of ST-X streak tube developed by Photek is 18 mm × 3 mm with a small size of Φ 93 mm × 145.8 mm. However, the edge spatial resolution is seriously deteriorated, while the center spatial resolution can reach 40 lp/mm [11]. The PV-201 streak tube developed by BIFO has a large effective photocathode area of 15 mm × 20 mm, but its spatial resolution is only 15 lp/mm [12]. The P510 streak tube developed by Photonis has a large effective area of 35 mm × 4 mm, but its spatial resolution is only 10 lp/mm and its size is larger than Φ 102 mm × 250 mm, which is not conducive to the miniaturization of the STIL [13]. Moreover, the 8200 streak tube developed by XIOPM has achieved a high spatial resolution of 20 lp/mm over the entire working area of Φ 28 mm. However, the magnification of the 8200 is 1, which results in a low luminance gain that is not conducive to the detection of weak light. It can be seen that spatial resolution and large detection area always contradict each other and are difficult to achieve at the same time. Since Gleckler first introduced a Multi-Slit Streak Tube Imaging Lidar (MS-STIL) in 2000, there have been several communities considering the number of slits that the photocathode can accommodate, the large-area photocathode, and high spatiotemporal resolution [14]. In 2002, Gelbart

DOI: 10.2478/msr-2023-0010
Corresponding author: shen@jit.edu.cn (L. Shen)

reported a MS-STIL with 16 slits and photocathode diameter of 25 mm [15]. Cao Xinbin designed a multi-slit streak tube with an effective photocathode area of Φ 17 mm and a spatial resolution of 25 lp/mm. Otherwise, the MS-STIL by Wenhao Li et al. uses a streak tube whose photocathode can accommodate 16 slits, but no specific information on spatiotemporal resolution has been reported [16]-[17]. In 2021, Shangwei Guo et al. reported a multispectral polarization streak tube imaging lidar with the number of photocathode slits being 16. However, the slit length is only 32 mm [18]. Therefore, the number of slits is positively correlated with the effective area of the photocathode and inversely proportional to the spatial resolution.

This article describes a general streak camera and gives experimental test results. In addition, a multi-slit miniaturized streak tube with a single-lens focusing system has been designed, which can greatly improve the detection field and accuracy of the STIL system, and can also image the dynamic target. Due to its ultra-small design, it can greatly reduce the size of the STIL system, which is expected to be reproduced in the UAV.

2. THE PRINCIPLE OF 3D IMAGING LIDAR

The principle of the STIL system is shown in Fig. 1, where the streak tube works in a single slit mode [19]. The laser pulse regulated by the emitting optical system is irradiated to the surface of the target, and the echo signal reflected by the target is emitted into the photocathode after filtering the stray light. The photon signal is converted into a photoelectric signal due to the external photoelectric effect. The spatial and temporal contour information of the optoelectronic signal can be regarded as a replica of the optical signal. In the streak tube, the photoelectrons are accelerated and focused under the action of the electromagnetic field. Then the photoelectrons entering the scanning field at different times in chronological order are deflected to the different spatial positions of the phosphor screen (from top to bottom, from left to right in space), so we can realize the conversion of ultrafast time signals to low-speed spatial image signals and complete the recording of time, space and light intensity information of the input signal. According to the full-screen time and temporal resolution, the axial detection distance and distance accuracy information can be calculated, and the transverse detection accuracy can be obtained according to the spatial resolution of the streak camera and the effective length of the cathode.

When the streak tube operates in multi-slit mode, the principle of STIL is the same as in single-slit mode, except that the photocathode receives a multi-slit image [15]. An optical fiber converter is placed in front of the photocathode, which can convert the two-dimensional spatial image reflected from the target into a one-dimensional slit image. The principle of the optical fiber converter is shown in Fig. 2 (16 slits for illustration). The received optical image is divided into 16 slit image sub-regions and each sub-region is divided into 16 × 16 pixels. Each pixel is coupled with an optical fiber. Thus, the input termination of 256 optical fibers formed by each pixel is connected to the radio-optical image, and the output is arranged in a row coupled to the slit of the multi-slit streak camera. 16 image sub-regions correspond to 16 slits. After being scanned by the streak tube, each slit represents a two-dimensional spatial image, and the image on the phosphor screen is captured by a CCD. In the end, the three-dimensional distance image and one-dimensional intensity image can be obtained by time inversion and image reconstruction.

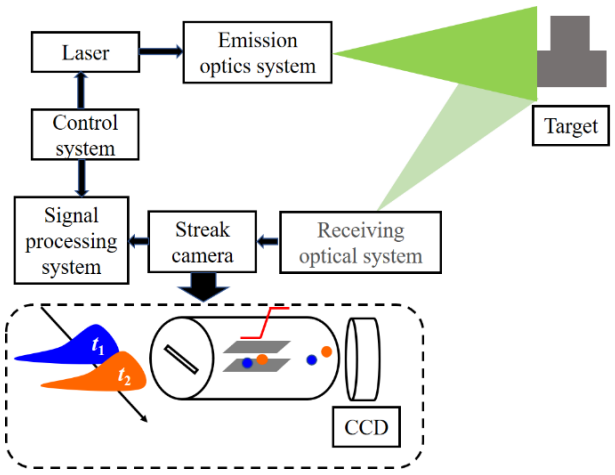

Fig. 1. The principle of the single-slit streak tube imaging lidar.

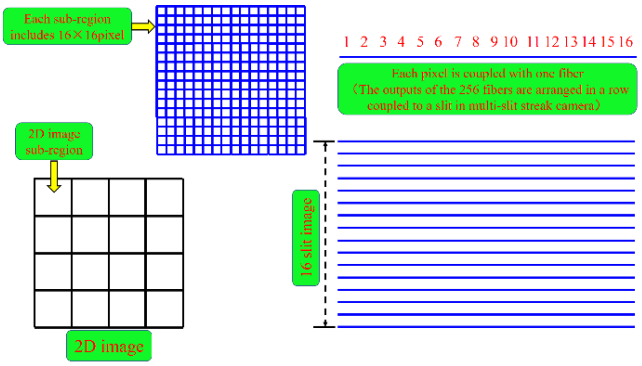

Fig. 2. The principle of light converter.

3. UNIVERSAL SINGLE-SLIT STREAK CAMERA

Fig. 3 shows a universal single-slit streak camera that can be used not only for STIL, but also for laser inertial confinement nuclear fusion, plasma physics, X-ray laser, and many other cutting-edge scientific fields to achieve the recording of ultrafast phenomena.

Fig. 3. A miniaturized streak camera.

Fig. 4 shows a miniaturized streak tube with high luminance gain, the core component of the miniaturized streak camera [20]. The streak tube uses a spherical cathode and screen structure design to achieve a large effective detection area of 35 mm × 3 mm. In the experiment, the USAF 1951 resolution board is used to evaluate the static spatial resolution, which is shown in Fig. 5. The sixth element of group four can be clearly distinguished, corresponding to a static spatial resolution of 28.5 lp/mm.

Fig. 4. A miniaturized streak tube with high luminance gain.

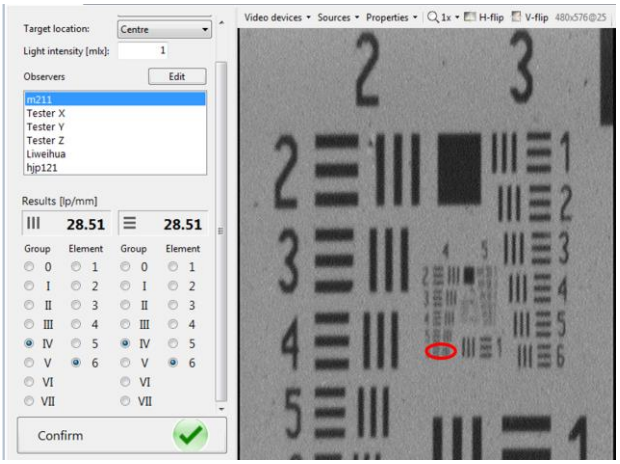

Fig. 5. Static spatial resolution under the USAF1951 Target.

Initial temporal resolution results of this streak camera were analyzed. The Full Width at Half Maximum (FWHM) method was used to calibrate the temporal resolution of this streak camera. The sequence pulses with 100 fs FWHM are generated by a 600 ps Fabry-Perot etalon. The CCD, which is used for recording the "streaking image" in the experiment has a pixel size of 2048 × 2048. The "streaking" image is shown in the embedded image in Fig. 6. Besides, the time integration curve along the sweeping direction for the red box selected in the embedded image is also represented by the black solid lines in Fig. 6. The temporal resolution was better than 58 ps (600 ps × 31/(1754-1433)), calculated from the two strongest curves.

The dynamic spatial resolution calibration was performed with the 5 ns full-screen time. A resolution board from Linear Target was set in front of the photocathode. It contains different resolutions of linear patterns from 4 lp/mm to 16 lp/mm. Fig. 7 shows the average intensity integration curve and the spatial resolution image of this streak camera. The spatial resolutions are defined by the Rayleigh criterion. The inset dotted lines are Gaussian fits of the linear image results, showing that the streak camera can achieve a dynamic spatial resolution higher than 10 lp/mm.

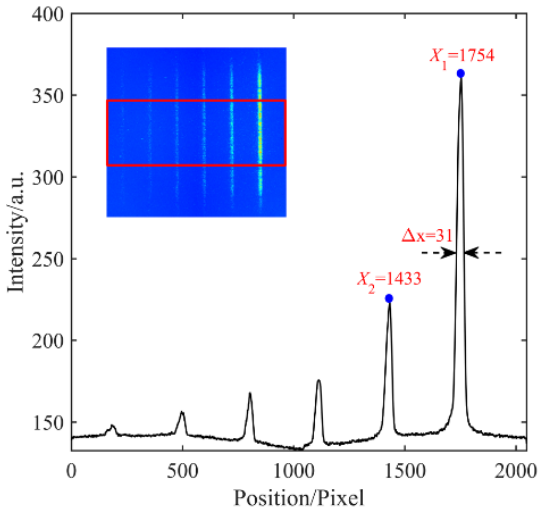

Fig. 6. Results of temporal resolution in the "streaking" mode.

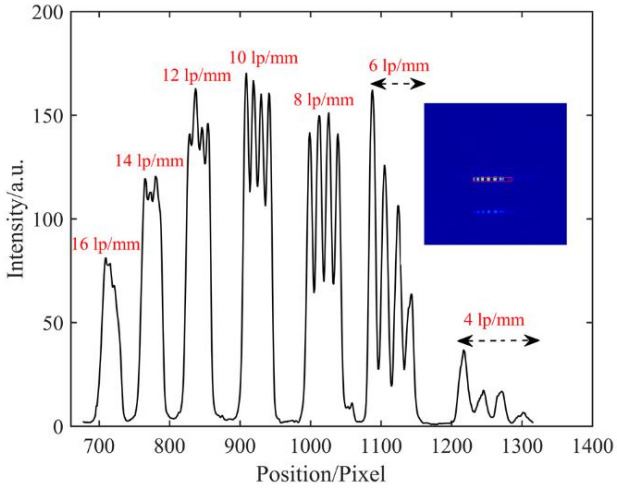

Fig. 7. Dynamic spatial resolution under the Linear Targets.

In the STIL system, the Photocathode Radiation Sensitivity (PRS) directly affects detection accuracy. In addition, the way the photocathode is manufactured seriously affects its PRS. When a non-transfer cathode system is used, it is difficult to fully process excess alkali. Over time, excess alkali metal is redistributed in the streak tube body, which will change the photocathode components, thereby resulting in a decrease in PRS. In addition, if the alkali metal material deposition is attached to the insulation layer of the high voltage component, it may cause creepage ignition and

shorten the life of the streak tube. Therefore, we use a transfer cathode system to manufacture the photocathode, minimizing the alkali metal contamination of the streak tube body components, and remove excess alkali metal baking. The production process avoids electrode contamination, which can effectively improve the sensitivity of the cathode and reduce noise. Fig. 8 shows the PRS test results. The PRS of the photocathode can reach 46 mA/W while the radiation wavelength is 500 nm.

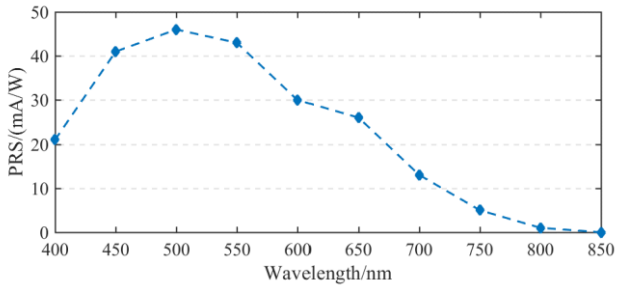

Fig. 8. PRS of the cathode.

4. A MULTI-SLIT MINIATURIZED STREAK TUBE DESIGN

A. *Electro-optical modelling*

The design of a large multi-slit photocathode area and high spatial resolution streak tube is of great significance for improving the detection accuracy of the STIL system. In this paper, a multi-slit large-format streak tube is modeled and simulated based on 3D Computer Simulation Technology Particle Studio (CST-PS), Finite Integral Technology (FIT), and the Monte Carlo (M-C) method [21]-[23]. The 3D electric field in the streak tube is calculated by resolving the discrete Maxwell's equations. To improve the accuracy of the calculations near the electrodes of the strong electric field, we use adaptive mesh refinement. The multi-slit miniaturized streak tube is designed with a single-lens focusing system [24]. The main structures include photocathodes, focusing systems, deflection systems, anodes, and phosphor screens, as shown in Fig. 9. The photocathode and phosphor screen have a spherical structure. On the one hand, this can reduce the aberration of the electron optical system, increasing the effective photocathode area and spatial resolution at the edge of the photocathode. On the other hand, the spherical structure can also reduce the temporal distortion and improve the screen image. Instead of the traditional immersion lens, a single-lens focusing system is used, which has better focusing ability. As the electron beam passes through a single-lens focusing system, the electrons appear to converge regardless of whether the intermediate potential is higher or lower than on either side. To improve the temporal resolution, the acceleration grid/mesh, which is introduced near the photocathode, causes the electrical breakdown and reduces the working stability of the streak tube. Another downside is that the accelerated electrodes described above intercept some of the photoelectrons (the photoelectron transmittance of the grid network is 60% to 70%) and reduce the photon efficiency of the streak tube. Therefore, to improve the stability and reliability, the streak tube designed in this paper uses a gridless/meshless structure.

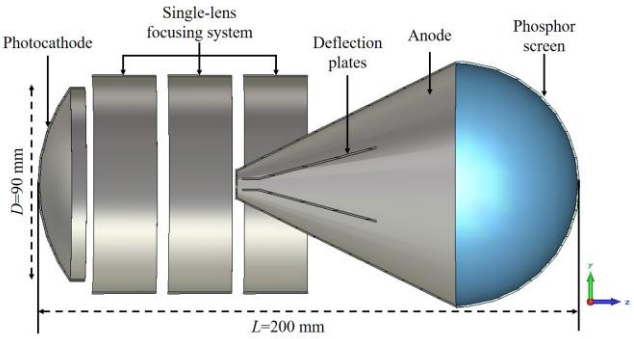

Fig. 9. A small-size streak tube model.

B. *Spatial resolution*

For coupling with the fiber converter, we calculate the spatial modulation transfer function in the square area of 36 mm × 36 mm, which is inserted into the effective photocathode area of Φ 50 mm. A set number of electrons are emitted 18 mm away from the photocathode along the scanning direction. The initial energy, launching elevation and azimuth of the electrons are determined by the Monte Carlo method. The electron pulses have a step length of 6 mm along the sagittal direction. According to the effective phosphor screen area and the deflection sensitivity, we set the static pre-bias voltage to ±750 V. The dynamic spatial modulation transfer function on the screen is calculated as shown in Fig. 10, while the full screen time is 668 ps. In the area of 36 mm × 36 mm, the dynamic spatial resolution of the streak tube can reach 12 lp/mm, and the number of pixels can reach $(36 \times 12)^2 \approx 432 \times 432$.

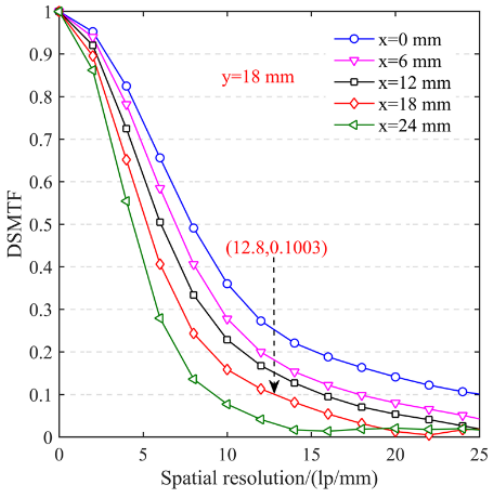

Fig. 10. Dynamic spatial resolution in slit direction (y = 18 mm).

C. *Temporal resolution*

To evaluate the temporal resolution of the multi-slit streak tube, three electron pulses with an interval of 50 ps and Full Width at Half Maximum (FWHM) of 1 ps are emitted at a distance of 18 mm (y = 18 mm) from the photocathode center. According to the effective area of the static phosphor screen, the deflection sensitivity and the full screen time, the scanning speed is set to 2.3×10^7 m/s. Fig. 11 shows the

distribution of the scanning electron pulses on the phosphor screen and the normalized distribution curve along the sagittal direction. Affected by the spatio-temporal dispersion, the electron pulse distribution reaching the phosphor screen has also dispersion in both the temporal and spatial axes. Obviously, there is overlap between adjacent electron pulses, mainly due to the electric field at the edge of the deflection plate. In addition, the red line represents the electron normalized intensity curve along the scanning direction. The valley bottom position probability is 0.3775, which is lower than the Rayleigh criterion of 0.7. Therefore, the temporal resolution of this multi-slit streak tube is better than 50 ps.

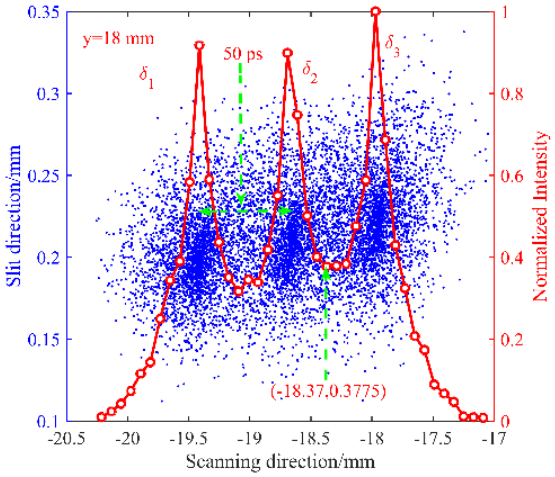

Fig. 11. Sweeping results of electron pulses with the interval of 50 ps.

D. Slit scanning image

To evaluate the imaging quality of multi-slit streak tubes, we tracked and analyzed the emission of 19 slit electrons 36 mm long from the photocathode. Fig. 12 shows the sweeping slit image of this multi-slit streak tube when the scanning speed is set to 0.08 *c*. Obviously, the electronic dusters of each slit do not overlap over the entire length of 36 mm and the boundaries are relatively clear. However, there is a slight bend at the image edges, which is mainly due to temporal distortion. As can also be seen from the figure, the magnification of this multi-slit streak tube is 1.

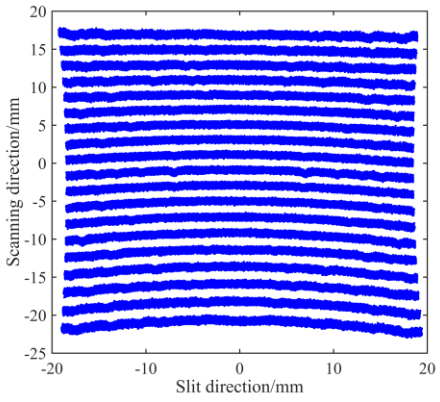

Fig. 12. Sweeping results of streaking electrons pulses.

Table 1. Performance parameters of the multi-slit streak tube.

Parameters	Value
Photocathode effective area (mm)	≥36 mm × 36 mm
Temporal resolution (ps)	<50
Spatial resolution (lp·mm^{-1})	≥12
Magnification	≈1
Phosphor screen area (mm)	≥
Working voltage (kV)	10~15
External dimensions (mm)	≤Φ 90 × 200

5. Conclusions

In this paper, we have presented a long-slit streak camera and designed a multi-slit streak tube suitable for the STIL detection system and the ICF experiment. The long-slit streak camera achieved a high static spatial resolution of 28.5 lp/mm over the entire effective photocathode area. The maximum value of PRS of this streak camera is 46 mA/W when the irradiation wavelength is 500 nm, which is a good detection performance for a visible imaging lidar system. In the experiment, we achieved a high dynamic spatial resolution of 10 lp/mm and a high temporal resolution of 58 ps. We also designed a multi-slit streak tube for dynamic target detection. The streak tube uses a spherically curved photocathode and screen to reduce image curvature and aberrations and increase spatio-temporal resolution. A single-lens focusing system is adopted to increase electrical stability and resistance. We have numerically evaluated the performance of this multi-slit streak tube. The results show that the dynamic spatial resolution can reach 12 lp/mm over the entire effective photocathode area of 36 mm × 36 mm. And the temporal resolution is better than 50 ps.

Acknowledgment

This study is supported by the Natural Science Foundation of the Jiangsu Higher Education Institutions of China (Grant No. 22KJD140003), the Ph.D. Project supported by the Jinling Institute of Technology (No. jit-b-202012).

References

[1] Sun, J., Liu, J., Wang, Q. (2015). Experimental research on multiple-slit streak tube imaging lidar. *Optik*, 126 (21), 3181-3184. https://doi.org/10.1016/j.ijleo.2015.07.077

[2] Wang, Q., Gao, J., Sun, J, Wei, J. (2012). A new method of detection of short scale ocean waves using a slit streak tube imaging lidar. In *2012 International Conference on Optoelectronics and Microelectronics*. IEEE, 182-184. https://doi.org/10.1109/ICoOM.2012.6316246

[3] Xia, W., Han, S., Ullah, N., Cao, J., Wang, L., Cao, J., Cheng, Y., Yu, H. (2017). Design and modeling of three-dimensional laser imaging system based on streak tube. *Applied Optics*, 56 (3), 487-497. https://doi.org/10.1364/AO.56.000487

[4] Hui, D., Luo, D., Tian, L., Lu, Y., Chen, P., Wang, J., Sai, X., Wen, W., Wang, X., Xin, L., Zhao, W., Tian, J. (2018). A compact large-format streak tube for imaging lidar. *Review Scientific Instrument*, 89 (4), 045113. https://doi.org/10.1063/1.5024269

[5] Tian, L., Shen, L., Li L., Wang, X., Chen, P., Wang, J., Chen, L., Zhao, W., Tian, J. (2021). Small-size streak tube with high edge spatial resolution. *Optik*, 242, 166791. https://doi.org/10.1016/j.ijleo.2021.166791

[6] Sun, J., Liu, J., Wang, Q. (2013). A multiple-slit streak tube imaging lidar and its detection ability analysis by flash lidar equation. *Optik*, 124 (3), 204-208. https://doi.org/10.1016/j.ijleo.2011.11.073

[7] Ye, G., Fan, R., Chen, Z., Yuan, W., Chen, D., He, P. (2016). Range accuracy analysis of streak tube imaging lidar systems. *Optics Communications*, 360, 7-14. https://doi.org/10.1016/j.optcom.2015.10.020

[8] Tian, J., Hui, D., Wang, T., Zhang, J., Chen, S., Jia, H. (2017). Small-size streak tube for imaging lidar. In *31st International Congress on High-Speed Imaging and Photonics*. SPIE 10328. https://doi.org/10.1117/12.2269063

[9] Hu, C., Niu, L., Yuan, Q., Wu, L., Yang, H., Yu, B. (2016). Research on 3D imaging based on streak tube imaging lidar. In *International Conference on Electronic Information Technology and Intellectualization (ICEITI 2016)*. DEStech Publications, 99-106. https://doi.org/10.12783/DTCSE%2FICEITI2016%2F6121

[10] Knight, F., Klick, D., Ryan-Howard, D., Theriault, J., Tussey, B., Beckman, A.M. (1989). Three-dimensional imaging using a single laser pulse. In *Laser Radar IV: Technical Symposium on Aerospace Sensing*. SPIE 1103, 174-189. https://doi.org/10.1117/12.960570

[11] Photek Company. "Citations of electronic resources." https://www.photek.com/streak-tubes/

[12] BIFO Company. "Citations of electronic resources." http://www.bifocompany.com

[13] Photonis Company. "Citations of electronic resources." www.photonis.com

[14] Gleckler, A. (2000). Multiple-slit streak tube imaging lidar (MS-STIL) applications. In *Laser Radar Technology and Applications V*. SPIE 4035, 266-278. https://doi.org/10.1117/12.397800

[15] Gelbart, A., Redman, B., Light, R., Schwartzlow, C., Griffis, A. (2002). Flash lidar based on multiple-slit streak tube imaging lidar. In *Laser Radar Technology and Applications VII*. SPIE 4723. https://doi.org/10.1117/12.476407

[16] Li, W., Guo, S., Zhai, Y., Han, S., Liu, F., Lai, Z. (2021). Occluded target detection of streak tube imaging lidar using image inpainting. *Measurement Science and Technology*, 32 (4), 045404. https://doi.org/10.1088/1361-6501/abd1b6

[17] Li, W., Guo, S., Zhai, Y., Liu, F., Lai, Z., Han, S. (2021). Target classification of multislit streak tube imaging lidar based on deep learning. *Applied Optics*, 60 (28), 8809-8817. https://doi.org/10.1364/AO.437470

[18] Guo, S., Li, W., Lai, Z., Meng, X., Han, S., Zhai, Y. (2021). Design and modeling of multi-spectral polarimetry streak tube imaging LiDAR. *Infrared Physics & Technology*, 118, 103872. https://doi.org/10.1016/j.infrared.2021.103872

[19] Gao, J., Sun, J., Wang, Q., Cong, M. (2017). 4-D imaging of the short scale ocean waves using a slit streak tube imaging Lidar. *Optik*, 136, 136-143. https://doi.org/10.1016/j.ijleo.2017.02.029

[20] Tian, L., Shen, L., Xue, Y., Chen, L., Li, L., Chen, P., Tian, J., Zhao, W. (2022). Theoretical and experimental research on spatial performances of the long-slit streak tube. *Measurement Science Review*, 22 (2), 58-64. https://doi.org/10.2478/msr-2022-0007

[21] Stoupin, S., MacPhee, A., Ose, N., MacDonald, M., Masse, L., Rusby, D., Schneider, M. (2022). A Monte Carlo technique to model performance of streak-camera-based time-resolving x-ray spectrometers. *Review of Scientific Instruments*, 93, 093510. https://doi.org/10.1063/5.0101705

[22] Computer Simulation Technology AG. "Citations of electronic resources." http://www.cst.com/

[23] Weiland, T. (2002). Advances in FIT/FDTD modeling. In *Proceedings of 18th Annual Review of Progress in Applied Computational Electromagnetics*.

[24] Tian, L., Shen, L., Chen, L., Li, L., Tian, J., Chen, P., Zhao, W. (2021). A new design of large-format streak tube with single-lens focusing system. *Measurement Science Review*, 21 (6), 191-196. https://doi.org/10.2478/msr-2021-0026

Received August 14, 2022
Accepted March 13, 2023